Polymer 50 (2009) 6281–6286

Contents lists available at ScienceDirect

Polymer

journal homepage: www.elsevier.com/locate/polymer

Physical and chemical modifications of thiol-ene networks to control activation energy of enthalpy relaxation

Junghwan Shin [a,*], Sergei Nazarenko [a], J. Paige Phillips [b], Charles E. Hoyle [a,b,1]

[a] School of Polymers and High Performance Materials, University of Southern Mississippi, 118 College Drive, Hattiesburg, MS 39406, USA
[b] Department of Chemistry and Biochemistry, University of Southern Mississippi, 118 College Drive, Hattiesburg, MS 39406, USA

ARTICLE INFO

Article history:
Received 2 September 2009
Accepted 22 October 2009
Available online 25 October 2009

Keywords:
Thiol-ene
Enthalpy relaxation
Activation energy

ABSTRACT

Gold nanoparticles and multi-functional acrylate (TMPTA) were incorporated into a photopolymerized thiol-ene (TMPMP–APE) network as a physical and chemical approach to intentionally control sub-T_g aging. The degree of the restriction effect was evaluated by differential cooling rate measurements allowing the quantification of the apparent activation energy for enthalpy relaxation (Δh^*) upon sub-T_g aging. Incorporation of gold nanoparticles (0.01 to 1 wt%) into the TMPMP–APE network increased T_g and decreased ΔC_p at T_g due to molecular mobility restrictions. The extent of enthalpy relaxation and apparent activation energy for enthalpy relaxation (Δh^*) clearly indicated the significant restrictive effect of the gold nanoparticles on the molecular mobility in the thiol-ene network. A TMPMP–APE–TMPTA ternary system was investigated in order to correlate Δh^* and network uniformity as a chemical approach. TMPTA, being capable of homopolymerization as well as TMPMP–TMPTA copolymerization, was incorporated into a TMPMP–APE network structure, thereby decreasing the network uniformity and significantly affecting the sub-T_g aging. The extent of enthalpy relaxation decreased and the distribution was drastically broadened as a function of TMPTA content due to molecular mobility restrictions, which were also quantified by measuring values for the apparent enthalpy relaxation activation energy (Δh^*).

1. Introduction

Thiol-ene photo-polymerization has attracted much attention as an emerging area in industry as well as academia as detailed in a review in 2004 [1]. The advantages of thiol-ene radical polymerization include initiatorless photo-polymerization, low oxygen inhibition, and versatility in hybridization with other thiol click type reactions that provide the potential for opening up many new applications [1–20]. In addition, the unique chemical reaction mechanism, i.e. free-radical step-growth, yields matrices with highly uniform network structure (Fig. 1(a)). The effect of thiol-ene network uniformity on physical/mechanical properties has been extensively studied and comparisons made with inhomogeneous multi-functional acrylate homopolymer networks (Fig. 1(b)) [5,6,21]. The uniform photopolymerized thiol-ene network structure is characterized by a very narrow glass transition region (FWHM ~ 10 °C). It is believed that this uniform network structures has very narrow spectrum of relaxation times and physical/mechanical properties are sensitive to environmental conditions, i.e. temperature.

Sub-T_g aging is a thermodynamic phenomenon involving volume and enthalpy relaxation upon annealing below the glass transition temperature of a polymer resulting in physical/mechanical property changes. Sub-T_g aging of thiol-ene photopolymerized networks with uniform chemical structure and a narrow distribution of relaxation times has been extensively investigated in terms of enthalpy relaxation by Shin et al. [22,23]. Thiol-ene networks showed temperature and time dependency relationships for enthalpy relaxation as generally observed in conventional polymers. However, the extent of enthalpy relaxation and overall relaxation rate significantly decreased with the rigidity of the ene chemical structures and functionality of the thiols forming thiol-ene networks. The effect of chemical and physical modification of thiol-ene network structure on enthalpy relaxation also has been reported. Overall both the rate and extent of enthalpy relaxation decreased by inclusion of flexible *n*-alkyl side chains as a function of alkyl chain length, while hydroxyl side chain incorporated into thiol-ene networks resulted in enhanced enthalpy relaxation. A multi-functional acrylate forming an inhomogeneous cross-linked structure by homopolymerization was copolymerized into thiol-ene networks to correlate enthalpy

---

* Corresponding author.
E-mail address: junghwan.shin@usm.edu (J. Shin).
[1] Sadly, Professor Charles E. Hoyle died during the preparation of this article.

0032-3861/$ – see front matter © 2009 Elsevier Ltd. All rights reserved.
doi:10.1016/j.polymer.2009.10.053

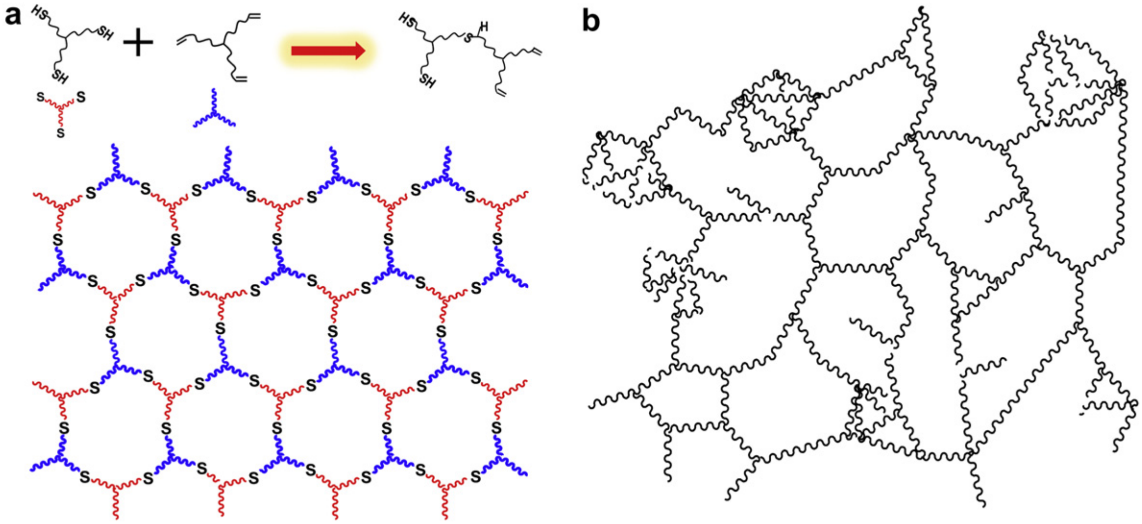

Fig. 1. (a) Uniform and dense network pictorial of photopolymerized thiol-ene made with trithiol and triene, and (b) inhomogeneous cross-linked pictorial of multi-acrylate homopolymer showing microgel formation.

relaxation and network uniformity. The extent and distribution of enthalpy relaxation of thiol-ene networks were significantly affected by disruption of the uniformity.

Because the rate of enthalpy/volume relaxation and corresponding rearrangement of polymer chains depend on the local environment surrounding mobile segments, sub-T_g aging can be restricted by various chemical and physical environmental effects such as thin films on substrates, the rigid amorphous regions of semi-crystalline polymers, highly cross-linked polymer networks, and nanocomposites [24–32]. In addition, the restriction of molecular mobility and enthalpy relaxation is directly related to configurational energy barriers in the relaxation process. Thus, the activation energy for the enthalpy relaxation (Δh^*) has been used to quantify the extent of the restrictive effect upon sub-T_g aging [32–39]. It has been reported that rigid chains and high crosslink density increase Δh^* [33–36]. Similarly, an increase in Δh^* of an epoxy matrix by incorporation of nano-clay due to the anchoring of epoxy chains to the nano-clay surface was also reported [32].

In the research described herein, gold nanoparticles and highly cross-linked TMPTA based rigid nano-domains as a physical and chemical approaches, respectively, were employed to control molecular relaxation dynamics upon sub-T_g aging. The restrictive effect on enthalpy relaxation was quantified by measuring values for the apparent enthalpy relaxation activation energy (Δh^*).

2. Experimental section

2.1. Materials

TMPMP Trimethylolpropane tri(3-mercapto-propionate), APE (allyl pentaerythritol), and TMPTA (trimethylolpropane triacrylate) were obtained from Bruno Bock Thio-Chemicals-S and Perstorp Specialty Chemicals, respectively. Gold nanopowder (99.9+%) was purchased from Aldrich. The structures of all components and corresponding acronyms are shown in the Chart 1. The photoinitiator, 2,2-dimethoxy 2-phenyl acetophenone (DMPA), was supplied by Ciba Specialty Chemicals. All materials were used as received.

Preparation of TMPMP–APE-gold and TMPMP–APE–TMPTA network films. TMPMP–APE-gold networks were prepared with gold dispersed in TMPMP and APE. Gold nanoparticles were added and dispersed in TMPMP with weight percents from 0.01 to 1.0. A detailed procedure for the dispersion of gold nanoparticles into TMPMP was described in the literature [43]. For TMPMP–APE–TMPTA ternary systems, the molar ratio of TMPTA to TMPMP–APE was varied from 0 to 100% to form TMPMP–APE–TMPTA ternary networks. 1 wt% of DMPA was first dissolve in gold nanoparticles dispersed TMPMP for TMPMP–APE-gold networks and TMPMP for TMPMP–APE–TMPTA ternary systems by sonication for 10 min. Thiol (–SH) and ene (–C=C–) concentrations were held constant at 1:1 functional group molar equivalent for all networks. Films were cast on glass plates (200 μm) and cured on a Fusion UV curing line system with a D bulb (400 W/cm^2) having a belt speed of 10 feet/min and irradiance of 3.1 W/cm^2. All samples were post-cured at 80 °C for 24 h to insure complete reaction and eliminate any possibility of chemical conversion effect on enthalpy relaxation during sub-T_g annealing.

2.2. Characterization

Glass transition temperatures and enthalpy relaxation for all modified thiol-ene networks were characterized with a TA Q1000 differential scanning calorimeter (DSC) with RCS 90 (Refrigerated

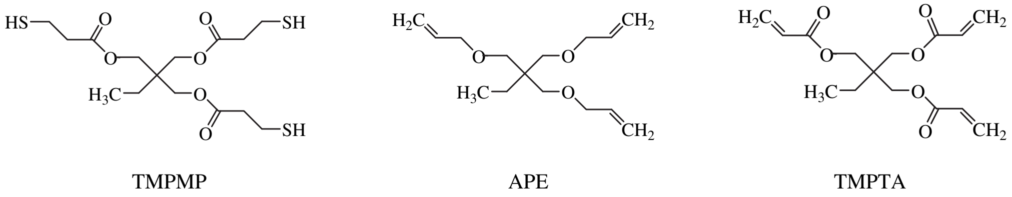

Chart 1. The molecular structures of thiol, ene, and acrylate.

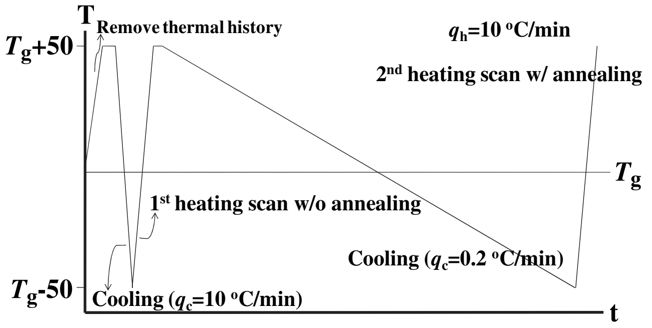

Fig. 2. Schematic representation of the differential cooling rate method. The symbols q_h and q_c represent heating/cooling rates.

Cooling System). A RCS 90 cooling head mounted on the DSC Q1000 furnace encases the DSC cell preventing frost build-up during operation. Three calibration steps (T_{zero} calibration, enthalpy constant calibration, and Temperature calibration) for the TA Q1000 were performed periodically. Detailed calibration protocol has been well described in previous reports [22]. For sub-T_g aging experiment, the differential cooling rate method was used as described in Fig. 2. The measurement was conducted twice and the sequence of cooling rate variation was reversed in the second running. Equivalent results were obtained in each case, i.e., instrumental drift did not play a factor, and the results were reproducible despite the different order for obtaining the data sets. Furthermore, the heat capacity of TMPMP–APE sample without aging, as a standard, was measured after every calibration and set of experiments to ensure consistency. All experiments were carried out under nitrogen with a flow rate of 50 mL/min. Sample weights were 8.0 ± 1.0 mg to ensure sufficient sensitivity for heat capacity measurements. DSC scans were conducted over the temperature range of ±50 °C from the glass transition region ($T_{g,i} \sim T_{g,e}$). Cooling rate (q_c) was differentiated at a fixed heating rate (q_h, 10 °C/min) to provide samples the different degree of non-equilibrium state in the glass and enthalpy recovery upon reheating. The detailed description of the experimental measurement technique is described in the text.

3. Results and discussion

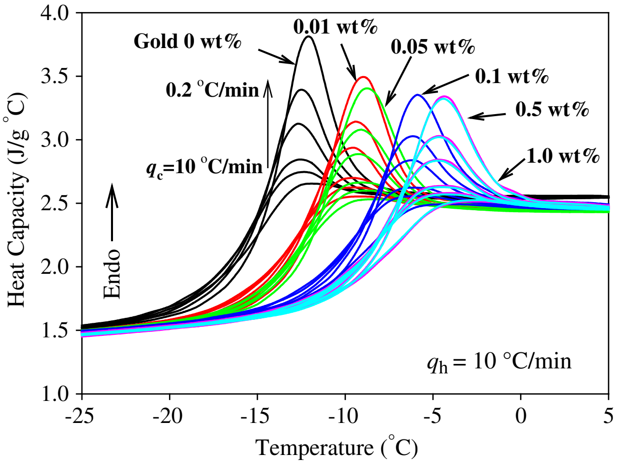

Fig. 3. DSC heating scans of TMPMP–APE-gold photopolymerized films after cooling with differential cooling rate (q_c).

The basic structural units used to make the thiol-ene and thiol-ene-acrylate ternary networks which are the subject of the investigation in this paper are shown in Chart 1 (gold structure is not shown). The three functional thiol (TMPMP) and ene (APE) are standard thiol and ene monomers typically used to make thiol-ene networks. Herein, we focus on defining the role of physically incorporated gold nanoparticles and chemical structure uniformity of the basic thiol-ene networks on sub-T_g aging behavior in terms of the apparent activation energy for enthalpy relaxation. The departure from equilibrium in the glassy state can be controlled via thermal treatment, i.e. by varying the cooling rate in DSC measurements. The cooling rate in DSC measurements. Hence, the thiol-ene networks were equilibrated above T_g to remove prior thermal history and cooled down at different cooling rate (q_c). The subsequent heat capacity was monitored upon reheating the sample through its glass transition. Equilibration achieved by maintaining the sample for 10 min. at a temperature above T_g ($T_{g,e}$ + 50 °C) effectively erases the previous thermal history, and is necessary to prepare the sample for sub-T_g aging. The differential cooling rate method measures the apparent activation energy for enthalpy relaxation and can potentially probe changes in enthalpy relaxation distribution.

TMPMP–APE-gold networks. The effect of gold nanoparticles on sub-T_g aging of thiol-Ene photopolymerized films was investigated as a physical approach to intentionally control enthalpy relaxation and molecular mobility by binding the network structure to a non-reactive nanoparticle additive. The TMPMP–APE-gold photopolymerized networks made from mixtures of TMPMP, APE, and dispersed gold nanoparticles (0.01–1 wt%) were analyzed by DSC with varying cooling rate (q_c) from 0.2 to 10 °C/min and a fixed heating rate (q_h = 10 °C/min). As shown in Fig. 3, with decreasing cooling rate, the intensity of the endothermic peak upon subsequent heating progressively increases for all TMPMP–APE-gold films. However, for results obtained at each cooling rate, the overall peak intensity of the subsequent heating scan decreases and T_g shifts to higher temperature as a function of gold nanoparticle content (Fig. 4). For reference, we note that the T_g values of the un-aged samples ($q_h = q_c$ = 10 °C/min) increase from −15 to −7 °C, leveling off at 0.5 wt% due to dispersion problems encountered in the pre-polymerized TMPMP and APE mixtures resulting in some aggregation of the gold nanoparticles as identified by light scattering [43]. Fig. 5 shows a plot of ΔC_p as a function of the gold nanoparticle wt% in the TMPMP–APE network. It is clear that restriction of

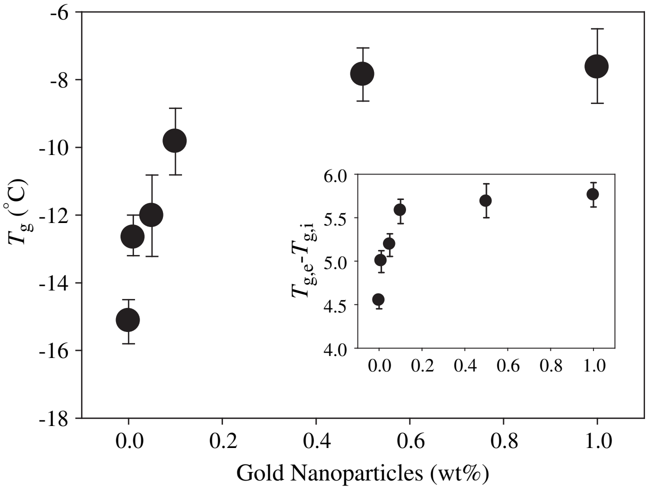

Fig. 4. Effect of gold nanoparticles on T_g of TMPMP–APE-gold photopolymerized films.

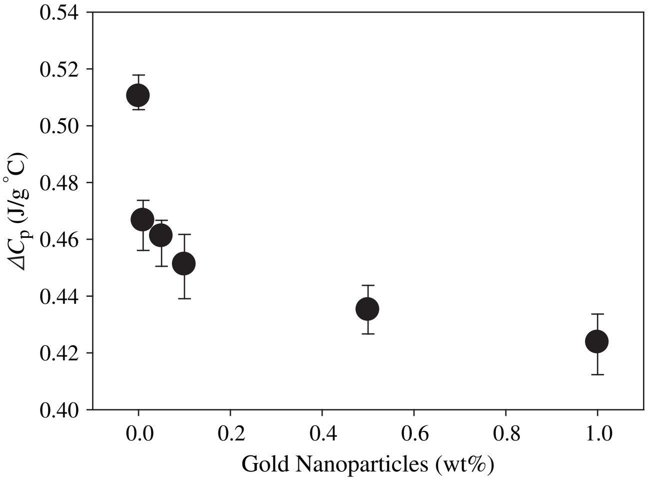

Fig. 5. Effect of gold nanoparticles on heat capacity of TMPMP–APE-gold photopolymerized films.

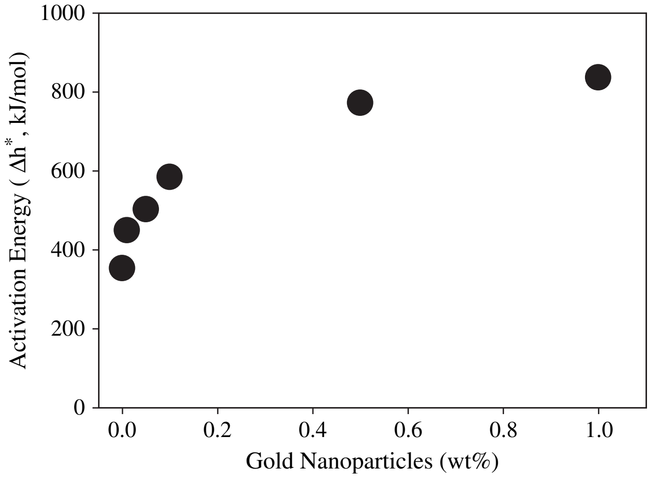

Fig. 7. Apparent activation energy (Δh^*) for enthalpy relaxation of TMPMP–APE-gold photopolymerized films as a function of gold nanoparticle content.

molecular mobility and hence lower ΔC_p in the rubbery phase upon incorporation of gold up to 0.5 wt% in the TriThiol–APE network is consistent with the T_g results in Fig. 4. This certainly results from a binding interaction between sulfide linkages (or un-reacted thiol groups) in the network structure and the gold surface which restricts molecular motion, raises the T_g, and correspondingly reduces ΔC_p at T_g. The gold nanoparticles effectively restrict conformational degrees of freedom otherwise operative in the TMPMP–APE network above T_g.

The logarithmic cooling rate (q_c) vs. reciprocal fictive temperature (T_f) for each of the TMPMP–APE-gold photopolymerized films are readily fit to straight lines with different slopes as shown in Fig. 6. The restriction of molecular relaxation can be mathematically quantified by the apparent activation energy for enthalpy relaxation (Δh^*) as defined in Eq. (1),

$$\frac{d(\ln q_c)}{d\left(1/T_f\right)} = -\frac{\Delta h^*}{R} \tag{1}$$

where R is the universal gas constant and q_c is cooling rate in DSC measurement [36–42]. The fictive temperature (T_f), which is defined as the temperature at which the extrapolation of thermodynamic parameters such as enthalpy, volume or entropy at a given temperature and annealing time in the glassy region intersects the extension of the liquid equilibrium line, can be used to characterize the structure of certain glassy states under a given set of conditions [44–46]. The apparent activation energy (Δh^*) obtained from the slopes in Fig. 6 increases from 353 kJ/mol for the neat Thiol-Ene network to 836 kJ/mol for the sample with 1 wt% gold nanoparticles in the network (Fig. 7). As with the T_g and ΔC_p results in Figs. 4 and 5, Δh^* increases substantially with an increase in gold nanoparticles up to approximately 0.5 wt%, whereupon aggregation of the gold nanoparticles occurs [43], thus limiting the gold surface area for interaction with the TMPMP–APE network. The increase in activation energy for enthalpy relaxation (Δh^*) is thus consistent with the reduction in the enthalpic departure from equilibrium with increasing gold concentration already noted.

TMPMP–APE–TMPTA ternary networks. TMPMP–APE–TMPTA ternary networks were next used to investigate the effect of network structural uniformity on sub-T_g aging. As reported in references [22,23], due to the network uniformity, TMPTA–APE has a very narrow glass transition temperature region and a distinct enthalpy relaxation peak around T_g obtained by DSC scanning of the pre-cooled sample at 10 °C/min cooling (q_c) followed by an

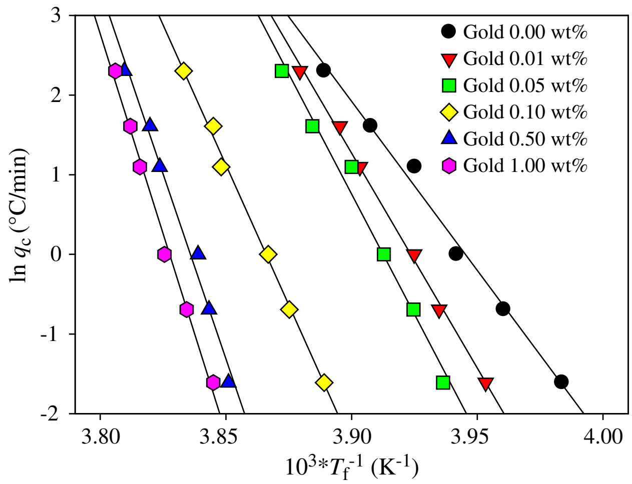

Fig. 6. Plots of logarithmic cooling rate (q_c) vs. reciprocal fictive temperature (T_f) of TMPMP–APE-gold photopolymerized films.

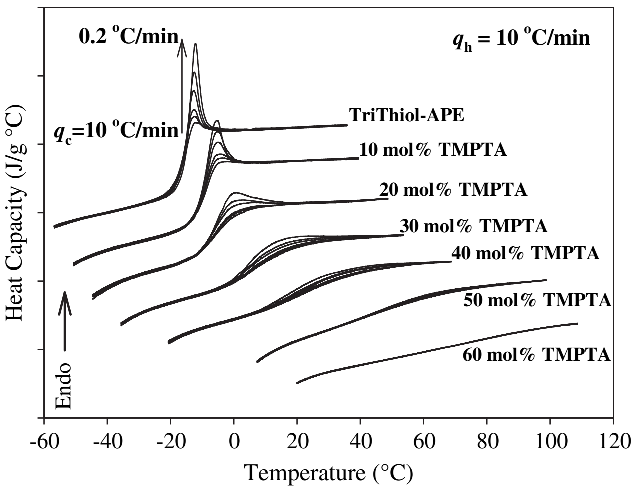

Fig. 8. DSC heating scans of photopolymerized TMPMP–APE–TMPTA ternary networks upon differential cooling rates (10, 5, 3, 1, 0.5, and 0.2 °C/min).

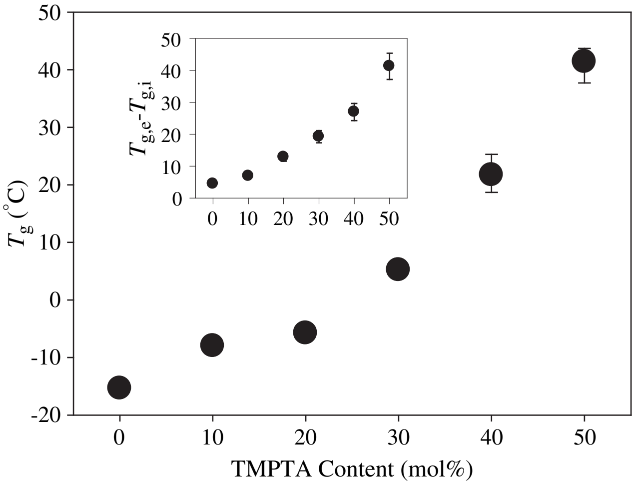

Fig. 9. Effect of TMPTA on T_g of photopolymerized TMPMP–APE–TMPTA ternary networks.

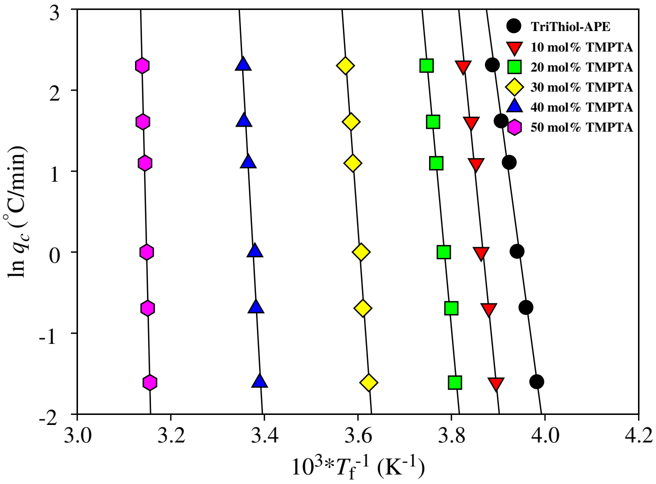

Fig. 11. Plots of logarithmic cooling rate (q_c) vs. reciprocal fictive temperature (T_f) of photopolymerized TMPMP–APE–TMPTA ternary networks.

immediate (no time for extended aging at a single annealing temperature) subsequent heating at a rate (q_h) of 10 °C/min. Concomitantly, photopolymerized TMPTA has an inhomogeneous cross-linked structure with a wide variation of crosslink densities and corresponding microgel structures, as well as dangling chain ends [47–52], resulting in a very broad glass transition region and no clearly defined enthalpy relaxation peak.

To define the effect of sub-T_g aging of ternary TMPTA–APE–TMPTA networks, systems were prepared by mixing TMPMP + APE with increasing TMPTA molar concentrations (10, 20, 30, 40, 50, and 60 mol%). The basic DSC glass transition temperature (see plots for $q_c = 10$ °C/min in Fig. 8) increases as a function of TMPTA content (Fig. 9), and the enthalpy relaxation peak is absent for TMPTA concentrations greater than 20%. It is clear that incorporating TMPTA into the TMPMP–APE network successfully decreases the network uniformity and microgel formation by TMPTA homopolymerization, acting like rigid amorphous region, restricts molecular mobility of thiol-ene networks, as previously reported [6,21,23].

The restriction of molecular mobility in the Thiol-Ene network by incorporation of the third component leads to a reduction of ΔC_p values. As shown in Fig. 10, ΔC_p at T_g of TMPMP–APE–TMPTA also significantly decreases as a function of TMPTA content due to restriction of internal degrees of freedom resulted from the microgelation of TMPTA accompanied by a broadened distribution of network/crosslink density and broad glass transition temperature range and distribution of relaxation times. The broadening of the temperature range and restrictive effect on enthalpy relaxation by incorporating TMPTA into the TMPMP–APE network is even more obvious when characterized by a differential cooling rate sub-T_g aging method (Fig. 8) from 0.2 to 10 °C/min at a fixed heating rate ($q_h = 10$ °C/min). This allows investigation of enthalpy relaxation behavior independent of temperature and time dependency, i.e., enthalpy relaxation distribution over a temperature range can be observed. In Fig. 8, the intensity of the endothermic peak progressively increases as the cooling rate decreases for all of the TMPMP–APE–TMPTA ternary systems, and the enthalpy relaxation peak maximum is lower as well as the distribution broadened with increasing TMPTA content. The apparent activation energy Δh^* from Eq. (1) obtained from slopes of linear regression lines in Fig. 11 (semi-log plots of cooling rate (q_c) vs. T_f^{-1}) increases from 349 kJ/mol for the neat TMPMP–APE network to 1962 kJ/mol for the network with 60 mol% of TMPTA in the TMPMP–APE–TMPTA ternary system (Fig. 12). This correlates with the decrease in the heat capacity

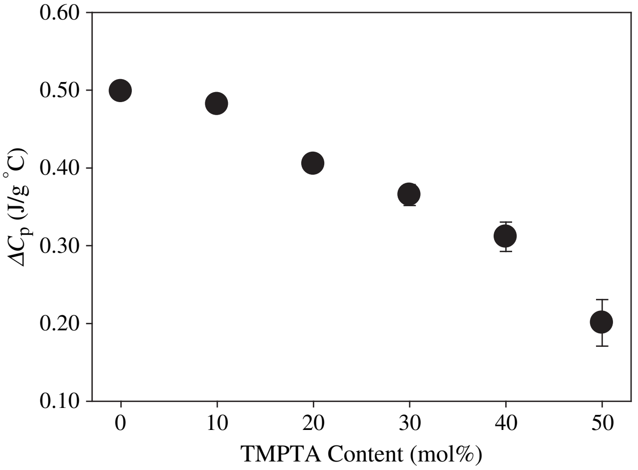

Fig. 10. Effect of TMPTA on heat capacity of photopolymerized TMPMP–APE–TMPTA ternary networks.

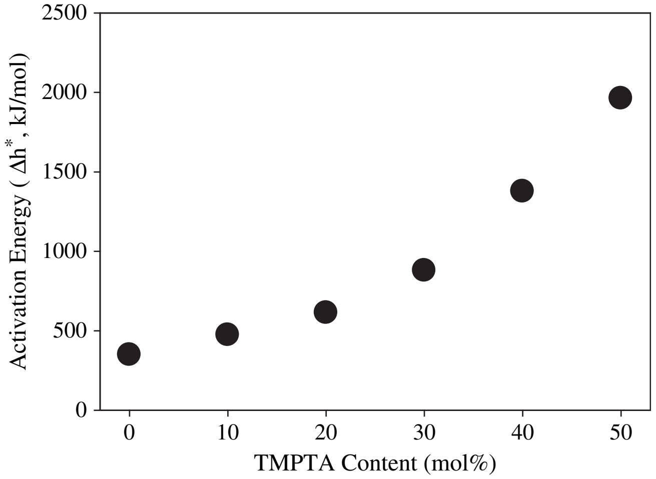

Fig. 12. Apparent activation energy (Δh^*) for enthalpy relaxation of photopolymerized TMPMP–APE–TMPTA ternary networks as a function of TMPTA content.

changes at T_g (ΔC_p) and clearly indicates that the enthalpy relaxation decreases with increasing TMPTA content.

4. Conclusions

Thiol-Ene networks were physically and chemically modified to provide control of apparent activation energy for enthalpy relaxation caused upon sub-T_g aging via two methods; addition of gold nanoparticles and chemical addition of a third (acrylate) component (ternary system). The effect of gold nanoparticles as a physical blending approach to reduce the extent of enthalpy relaxation on TMPMP–APE network was first demonstrated. The decrease in the amount of relaxed enthalpy upon sub-T_g aging, increase in T_g, decrease in ΔC_p, and increase in Δh^* all occur with an increase in the gold nanoparticle content and attain limiting values at a gold nanoparticles concentration of 0.5 wt%. Effective incorporation of higher gold content at levels of 1 wt% or greater will require new mixing protocols due to the tendency for aggregation. Multifunctional acrylate (TMPTA) was incorporated into a TMPMP–APE network structure as a chemical approached to investigate the effect of the network uniformity on the apparent activation energy for enthalpy relaxation. The extent of enthalpy relaxation decreased and the distribution was drastically broadened as a function of TMPTA content. It can be concluded that network uniformity manipulated by chemical structural change is responsible for manipulation of the activation energy for enthalpy relaxation, i.e. sub-T_g relaxation of TMPMP–APE based networks. The restrictive effect of inorganic gold nanoparticles and rigid amorphous regions due to microgelation of TMPTA homopolymerization successfully decreases segmental chain mobility of TMPMP–APE networks resulting in significant reduction of activation energy for enthalpy relaxation. The physical and chemical approaches demonstrated for the model thiol-ene network provides a guide for control and restriction of sub-T_g aging of polymer networks.

Acknowledgements

We acknowledge Perstorp, Bruno Bock and Ciba Specialty Chemicals for materials, and Fusion UV Systems for the light source.

References

[1] Hoyle CE, Lee TY, Roper T. J Polym Sci Part A Polym Chem 2004;42:5301.
[2] Cramer NB, Bowman CN. J Polym Sci Part A Polym Chem 2001;39:3311.
[3] Cramer NB, Reddy SK, Cole M, Hoyle CE, Bowman CN. J Polym Sci Part A Polym Chem 2004;42:5817.
[4] Khire VS, Harant AW, Watkins AW, Anseth KS, Bowman CN. Macromolecules 2006;39:5081.
[5] Senyurt AF, Hoyle CE, Wei H, Piland SG, Gould TE. Macromolecules 2007;40:3174.
[6] Wei H, Senyurt AF, Jönsson S, Hoyle CE. J Polym Sci Part A Polym Chem 2007;45:822.
[7] Roper TM, Guymon CA, Jönsson ES, Hoyle CE. J Polym Sci Part A Polym Chem 2004;42:6283.
[8] Lee TY, Roper TM, Jönsson ES, Guymon CA, Hoyle CE. Macromolecules 2004;37:3606.
[9] Li Q, Zhou H, Wicks DA, Hoyle CE. J Polym Sci Part A Polym Chem 2007;45:5103.
[10] Wei H, Li Q, Ojelade M, Madbouly S, Otaigbe JU, Hoyle CE. Macromolecules 2007;40:8788.
[11] Senyurt AF, Warren G, Whitehead JB, Hoyle CE. Polymer 2006;47:2741.
[12] Moran IW, Briseno AL, Loser S, Carter KR. Chem Mater 2008;20:4595.
[13] Yi YW, Khire V, Bowman CN, Maclennan JE, Clark NA. J Appl Phys 2008;103:6.
[14] Good BT, Reddy S, Davis RH, Bowman CN. Sens Actuators B Chem 2007;120:473.
[15] Pojman JA, Varisli B, Perryman A, Edwards C, Hoyle CE. Macromolecules 2004;37:691.
[16] Khire VS, Benoit DSW, Anseth KS, Bowman CN. J Polym Sci Part A Polym Chem 2006;44:7027.
[17] Khire VS, Lee TY, Bowman CN. Macromolecules 2008;41:7440.
[18] Dickey MD, Collister E, Raines A, Tsiartas P, Holcombe T, Sreenivasan SV, et al. Chem Mater 2006;18:2043.
[19] Fox AE, Fontecchio AK. Appl Phys Lett 2007;91:3.
[20] Campos LM, Meinel I, Guino RG, Scheirhorn M, Gupta N, Stucky GD, et al. J Adv Mater 2008;20:3728.
[21] Senyurt AF, Wei H, Phillips B, Cole M, Nazarenko S, Hoyle CE, et al. Macromolecules 2006;39:6315.
[22] Shin J, Nazarenko S, Hoyle CE. Macromolecules 2008;41:6741.
[23] Shin J, Nazarenko S, Hoyle CE. Macromolecules 2009;42:6549.
[24] Forrest JA, Dalnoki-Veress K. Adv Colloid Interface Sci 2001;94:167.
[25] Zhu L, Cheng SZD, Calhoun BH, Ge Q, Quirk RP, Thomas EL, et al. J Am Chem Soc 2000;122:5957.
[26] Nogales K, Ezquerra TA, Batallan F, Frick B, Lopez-Cabarcos E, Balta-Calleja FJ. Macromolecules 1999;32:2301.
[27] Dobbertin J, Hannemann J, Schick C, Potter M, Dehne H. J Chem Phys 1998;108:9062.
[28] Zhao J, Wang J, Li C, Fan Q. Macromolecules 2002;35:3097.
[29] Zhukov S, Geppert S, Stuhn B, Staneva R, Ivanova R, Gronski W. Macromolecules 2002;35:8521.
[30] Jackson CL, McKenna GB. Rubber Chem Technol 1991;64:760.
[31] Barut G, Pissis P, Pelster R, Nimtz G. Phys Rev Lett 1998;80:3543.
[32] Lu H, Nutt S. Macromolecules 2003;36:4010.
[33] Karasz FE, MacKnight WJ. Macromolecules 1968;1:537.
[34] Shen MC, Eisenberg A. Rubber Chem Technol 1970;43:95.
[35] Cheng SZD, Heberer DP, Janimak JJ, Lien SHS, Harris FW. Polymer 1991;32:2053.
[36] Hutchinson JM. Prog Polym Sci 1995;20:703.
[37] Hutchinson JM, Kumar P. Thermochim Acta 2002;391:197.
[38] Pan P, Zhu B, Inoue Y. Macromolecules 2007;40:9664.
[39] Qin Q, McKenna GB. J Non-crystal Sol 2006;352:2977.
[40] Montserrat S, Calventus Y, Hutchinson JM. Prog Org Coat 2006;55:35.
[41] Calventus Y, Montserrat S, Hutchinson JM. Polymer 2001;42:7081.
[42] Cortes P, Montserrat S, Hutchinson JM. J Appl Polym Sci 1997;63:17.
[43] Phillips JP, Mackey NM, Confait BS, Heaps DT, Deng X, Todd ML, et al. Chem Mater 2008;20:5240.
[44] Ritland HN. J Am Ceram Soc 1954;37:370.
[45] Moynihan CT, Easteal AJ, DeBolt MA. J Am Ceram Soc 1976;59:12.
[46] Mathot VBF. Calorimetry and thermal analysis of polymers. New York: Hanser; 1994.
[47] Boots HMJ, Kloosterboer JG, van de Hei GMM. Br Polym J 1985;17:219.
[48] Elliott JE, Bowman CN. Macromolecules 1999;32:8621.
[49] Lovestead TM, Bowman CN. Macromolecules 2005;38:4913.
[50] Kloosterboer JG, Lijten GFCM, Boots HMJ. Makromol Chem Macromol Symp 1989;24:223.
[51] Bowman CN, Anseth KS. Macromol Symp 1995;93:269.
[52] Kannurpatti AR, Anseth JW, Bowman CN. Polymer 1998;39:2507.